VIP Catalyst Stability | Very Important Paper

DOI: 10.1002/anie.201308245

Stabilization of Copper Catalysts for Liquid-Phase Reactions by Atomic Layer Deposition**

*Brandon J. O'Neill, David H. K. Jackson, Anthony J. Crisci, Carrie A. Farberow, Fengyuan Shi, Ana C. Alba-Rubio, Junling Lu, Paul J. Dietrich, Xiangkui Gu, Christopher L. Marshall, Peter C. Stair, Jeffrey W. Elam, Jeffrey T. Miller, Fabio H. Ribeiro, Paul M. Voyles, Jeffrey Greeley, Manos Mavrikakis, Susannah L. Scott, Thomas F. Kuech, and James A. Dumesic**

Abstract: *Atomic layer deposition (ALD) of an alumina overcoat can stabilize a base metal catalyst (e.g., copper) for liquid-phase catalytic reactions (e.g., hydrogenation of biomass-derived furfural in alcoholic solvents or water), thereby eliminating the deactivation of conventional catalysts by sintering and leaching. This method of catalyst stabilization alleviates the need to employ precious metals (e.g., platinum) in liquid-phase catalytic processing. The alumina overcoat initially covers the catalyst surface completely. By using solid state NMR spectroscopy, X-ray diffraction, and electron microscopy, it was shown that high temperature treatment opens porosity in the overcoat by forming crystallites of γ-Al_2O_3. Infrared spectroscopic measurements and scanning tunneling microscopy studies of trimethylaluminum ALD on copper show that the remarkable stability imparted to the nanoparticles arises from selective armoring of under-coordinated copper atoms on the nanoparticle surface.*

Precious metal catalysts are used extensively in the petrochemical industry. Although it would be desirable to replace precious metal catalysts (e.g., Pt) with base metals that are more earth-abundant (e.g., Cu), base metal catalysts are susceptible to irreversible deactivation through sintering and/or leaching under liquid-phase conditions.[1] Irreversible deactivation of a catalyst is a significant impediment for a practical catalytic process, as replacement of a deactivated catalyst can be expensive, require lengthy process shutdowns, and create solid waste that requires reprocessing. Accordingly, the search for base metal catalysts that are stable under liquid-phase reaction conditions remains an important challenge in the field of heterogeneous catalysis.

Herein, we report a method to stabilize copper nanoparticles on γ-Al_2O_3 by atomic layer deposition (ALD) of an alumina overcoat. Although ALD has been shown to inhibit nanoparticle mobility of precious metal catalysts under gas-phase conditions, this is the first report that ALD can stabilize a base metal catalyst for liquid-phase catalytic processing. By combining kinetic studies, advanced-materials characterization, and first-principles calculations, we elucidate how the overcoat provides stability to the nanoparticles without appreciably affecting the reaction kinetics for our probe reaction.

[*] B. J. O'Neill, Dr. A. J. Crisci, C. A. Farberow, Dr. A. C. Alba-Rubio, Prof. M. Mavrikakis, Prof. T. F. Kuech, Prof. J. A. Dumesic
Department of Chemical and Biological Engineering
University of Wisconsin
Madison, WI 53706 (USA)
E-mail: dumesic@engr.wisc.edu

D. H. K. Jackson, F. Shi, Prof. P. M. Voyles, Prof. T. F. Kuech
Materials Science Program, University of Wisconsin
Madison, WI 53706 (USA)

Dr. A. J. Crisci, Prof. S. L. Scott
Department of Chemistry & Biochemistry, University of California
Santa Barbara, CA 93106 (USA)

Dr. J. Lu
Department of Chemical Physics
University of Science and Technology of China
Hefei, 230026 (China)

Dr. P. J. Dietrich, Dr. X. Gu, Prof. F. H. Ribeiro, Prof. J. Greeley
Department of Chemical Engineering, Purdue University
West Lafayette, IN 47907 (USA)

Dr. C. L. Marshall, Prof. P. C. Stair, Dr. J. T. Miller
Chemical Science and Engineering, Argonne National Laboratory
Argonne, IL 60439 (USA)

Prof. P. C. Stair
Department of Chemistry, Northwestern University
Evanston, IL 60208 (USA)

Dr. J. W. Elam
Energy Systems Division, Argonne National Laboratory
Argonne, IL 60439 (USA)

[**] This material is based upon work supported as part of the Institute for Atom-efficient Chemical Transformations (IACT), an Energy Frontier Research Center funded by the U.S. Department of Energy, Office of Science, Office of Basic Energy Sciences. Electron microscopy was supported by the U.S. Department of Energy (DOE), Office of Basic Energy Sciences (DE-FG02-99ER45777). Chemisorption/kinetics were supported by the U.S. Department of Energy (DOE), Office of Basic Energy Sciences (DE-FG02-84ER13183). NMR was supported by the National Science Foundation (NSF) under the Center for Enabling New Technologies through Catalysis (CENTC) and used the Materials Research Laboratory, supported by the MRSEC Program of the NSF (DMR05-20415). Use of the Advanced Photon Source was supported by the U.S. DOE (DE-AC02-06CH11357). MRCAT operations are supported by DOE and the MRCAT member institutions. Some computational work was performed using resources from the Pacific Northwest National Laboratory and the National Energy Research Scientific Computing Center.

Supporting information for this article, including of details of the synthesis, kinetic measurements, characterization, and computational techniques, is available on the WWW under http://dx.doi.org/10.1002/anie.201308245.

ALD is a self-limiting growth process that creates highly conformal coatings.[4] In this work, the ALD overcoats were deposited onto oxidized copper nanoparticles that were synthesized by incipient wetness impregnation of γ-Al_2O_3. The catalyst was reduced under a flow of H_2 and passivated in dilute O_2 (Figure 1a), before the overcoat was deposited using 45 cycles of alternating exposure to trimethylaluminum (TMA) and water, leaving the metal nanoparticles encapsulated in an amorphous alumina overcoat (Figure 1b). Treatment at 973 K produced porosity in the overcoat, thereby providing access to the underlying copper particles (Figure 1c).

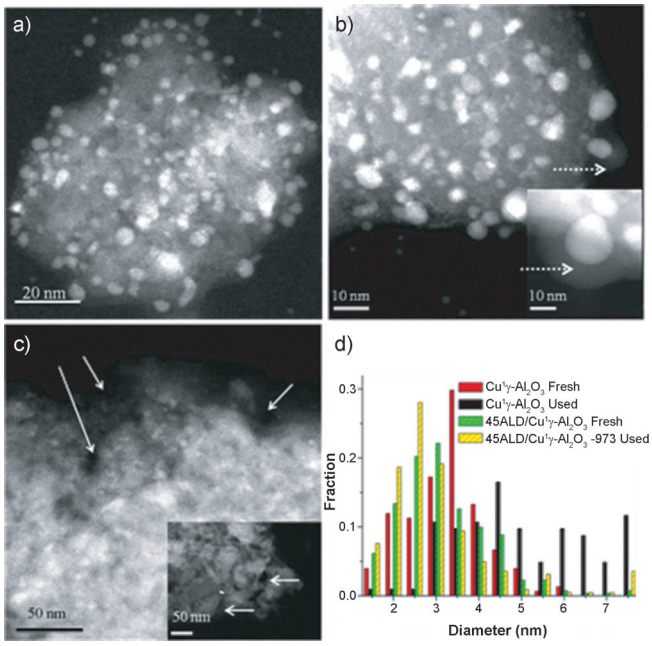

Figure 1. a–c) STEM images of Cu/γ-Al_2O_3 (a), 45ALD/Cu/γ-Al_2O_3 (b), and 45ALD/Cu/γ-Al_2O_3-973 (c). d) Particle size distributions of fresh and used catalysts. Dashed arrows point to the ALD overcoat, and solid arrows indicate pores in the overcoat.

Prior to ALD overcoating, the total surface area of the copper supported on γ-Al_2O_3 (Cu/γ-Al_2O_3, 5.9 wt%) was 190 $m^2 g^{-1}$, and the total pore volume was 0.45 $cm^3 g^{-1}$ (Supporting Information, Table S1). After reduction in H_2 at 573 K, Cu/γ-Al_2O_3 had 86 $\mu mol\, g^{-1}$ of surface Cu^0 sites, as titrated by N_2O flow chemisorption.[5] The surface area and pore volume of ALD-overcoated samples (45ALD/Cu/γ-Al_2O_3, 2.5 wt%) decreased (16 $m^2 g^{-1}$, 0.03 $cm^3 g^{-1}$), which indicates that the ALD process filled the pores of the support and created a continuous overcoat. Additionally, Cu^0 sites were not detected by N_2O titration after reduction in H_2 at 573 K. In contrast, following treatment at 973 K (45ALD/Cu/γ-Al_2O_3-973) in air, the surface area and pore volume increased (39 $m^2 g^{-1}$, 0.08 $cm^3 g^{-1}$), which suggests pore formation in the overcoat. Importantly, treatment at 973 K followed by H_2 reduction re-exposed Cu^0 surface sites (23 $\mu mol\, g^{-1}$). The chemisorption and surface-area measurements corroborate observations of the overcoat (Figure 1b) and pore formation (Figure 1c) from scanning transmission electron microscopy (STEM).

The catalytic properties of Cu/γ-Al_2O_3 and 45ALD/Cu/γ-Al_2O_3-973 were studied for the liquid-phase hydrogenation of furfural to furfuryl alcohol in 1-butanol as the solvent (403 K, 22 bar H_2). This reaction was chosen as an example of an industrially relevant copper-catalyzed hydrogenation that would benefit from stabilized copper catalysts.[6] Furthermore, furfural is derived from the hemicellulose portion of biomass, and its importance is expected to increase as industries move to renewable feedstocks. The deactivation of Cu/γ-Al_2O_3 during a reaction in a continuous flow reactor is shown in Figure 2a. Deactivation by the deposition of carbonaceous species (i.e., coke) on the catalyst is reversible upon calcination, whereas deactivation by leaching or sinter-

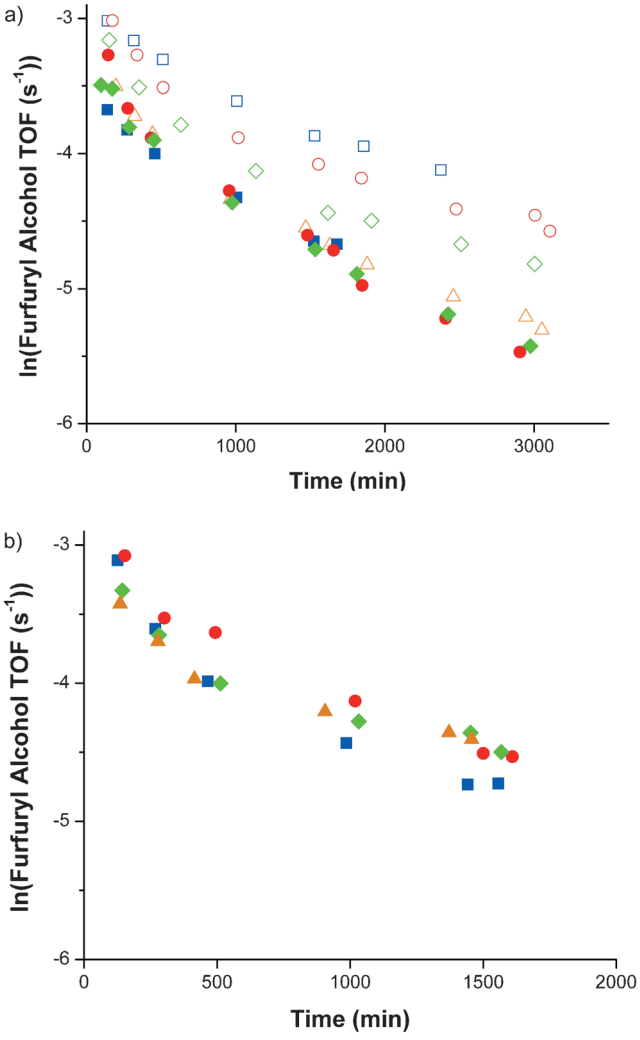

Figure 2. a) Furfural hydrogenation in liquid butanol at 403 K and 22 bar H_2 using Cu/γ-Al_2O_3 (fresh □; one regeneration ○; two regenerations ◇; three regenerations △) and 45ALD/Cu/γ-Al_2O_3-973 (fresh ■; one regeneration ●; two regenerations ◆). b) Furfural hydrogenation in liquid water using 45ALD/Cu/γ-Al_2O_3-973 (fresh ■; one regeneration ●; two regenerations ◆; three regenerations ▲) at 403 K and 22 bar H_2. The TOF was calculated using the number of sites of fresh, unused catalyst.

ing of copper is irreversible. The deactivation of Cu/γ-Al_2O_3 (Figure 2a, open symbols) is not fully reversed by calcination followed by reduction in H_2, which suggests that sintering and leaching have occurred.

STEM was used to measure the particle size distribution of the copper nanoparticles before and after the reaction to confirm sintering. The size of the Cu/γ-Al_2O_3 particles was 3 ± 1 nm before the reaction and increased to 5 ± 2 nm after three cycles of reaction and regeneration (Figure 1d). The copper loading of Cu/γ-Al_2O_3, which was analyzed by inductively coupled plasma atomic emission spectroscopy (ICP-AES), was 5.9 ± 0.2% before the reaction and 5.0 ± 0.2% after three cycles of reaction and regeneration, which indicates that leaching of copper from the catalyst has occurred.

The stability of 45ALD/Cu/γ-Al_2O_3-973 differs substantially from that of Cu/γ-Al_2O_3 under the same reaction and regeneration conditions. The initial activity of 45ALD/Cu/γ-Al_2O_3-973 was fully recovered after calcination and re-reduction (Figure 2a, filled symbols). The particle size was 3 ± 1 nm before and after three cycles of reaction with intermediate regeneration (Figure 1d), which confirms that the overcoat prevented sintering. Furthermore, the copper loading of the catalyst, which was measured by ICP-AES, was 2.4 ± 0.1% before the reaction and 2.5 ± 0.1% after the reaction, which suggests that the overcoat prevented copper leaching. (The loading of 45ALD/Cu/γ-Al_2O_3-973 is lower due to the mass of alumina added by ALD.) Also, in a control experiment, the Cu/γ-Al_2O_3 catalyst without an ALD overcoat exhibited irreversible deactivation after calcination at 973 K (Figure S1), which demonstrates that the overcoat, not the calcination at high temperature, is responsible for the stability of 45ALD/Cu/γ-Al_2O_3-973. Notably, the ALD overcoat stabilizes the copper nanoparticles against sintering and leaching even in the corrosive environment of high-temperature liquid water (Figure 2b). The overcoat did not affect the selectivity of the hydrogenation under the reaction conditions of this study, as furfuryl alcohol was the only hydrogenation product observed.

Solid state ^{27}Al magic-angle spinning (MAS) NMR spectroscopy and powder X-ray diffraction (XRD) were employed to probe the mechanism of pore formation. Alumina was deposited on copper that was supported on TiO_2 (45ALD/Cu/TiO_2, Figure 3a) to eliminate signals from the support and to more clearly demonstrate the restructuring of the overcoat (see Table S2 and Figure S2 for 45ALD/Cu/γ-Al_2O_3). Figure 3a shows that 6-, 5-, and 4-coordinate aluminum atoms are present in the overcoat (resonances at 9.3, 33.3, and 65.5 ppm). The presence of 5-coordinate aluminum is consistent with the amorphous nature of the overcoat before calcination.[7] After calcination at 973 K, the resonance corresponding to 5-coordinate aluminum disappears, and the ratio of 6- to 4-coordinate aluminum suggests crystallization.[8] Results from XRD (Figure 3b) show that the overcoat begins to crystallize during heating at 973 K, as confirmed by reflections from γ-Al_2O_3. The crystallization creates voids in the overcoat as it becomes more dense, thus exposing the underlying copper atoms.[9] Interestingly, the ALD overcoat also stabilizes the TiO_2 support, preventing its reorganization from anatase to rutile (Figure S3).[10]

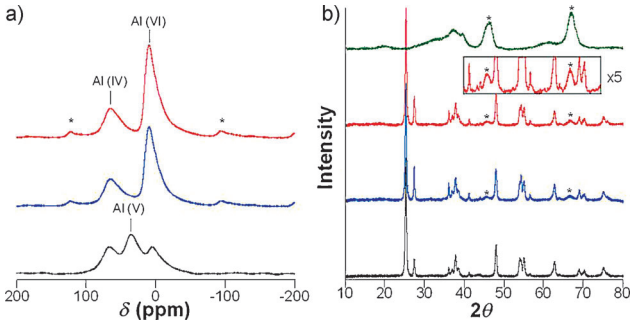

Figure 3. a) Solid-state ^{27}Al MAS-NMR spectra of 45ALD/Cu/TiO_2 before (——) and after calcination at 973 K for 2 h (——) and 4 h (——). Spinning sidebands are indicated by *. b) Powder X-ray diffraction patterns for γ-Al_2O_3 (——) and 45ALD/Cu/TiO_2 before (0 h, ——) and after calcination (2 h ——; 4 h ——). A magnified spectrum for 45ALD/Cu/TiO_2 (5×) is also shown, highlighting γ-Al_2O_3. γ-Al_2O_3 peaks are indicated by *.

Sintering and leaching of metal nanoparticles are believed to originate from under-coordinated copper atoms located at edges, corners, and defects.[11] Accordingly, stability imparted to the copper nanoparticles by ALD overcoating may result from selective interactions of the overcoat with under-coordinated copper atoms that remain after pore opening.[3,12] Scanning tunneling microscopy (STM) on a Cu(111) surface was used to probe the interactions of alumina with the surface and to observe nanoscale changes of the ALD alumina after high-temperature treatment. Alumina clusters were observed on the surface of a pre-oxidized and hydrated (i.e., exposed to air and then water) Cu(111) surface after four cycles of alternating exposure to TMA and water (Figure 4a). The height profile line scans in Figure 4c and d (corresponding to the blue lines in Figure 4a and b) indicate that alumina preferentially decorated the step edges and defects of the Cu(111) surface. After four cycles, alumina occupied 59 ± 3% of the terrace sites and 91 ± 1% of the edge and defect sites. When this surface was heated to 773 K under ultra-high vacuum, the coverage of Cu(111) terraces decreased relative to that of the edges (30 ± 4% of terraces vs. 80 ± 3% of edges and defects; Figure 4b). These results support the hypothesis that alumina preferentially binds to under-coordinated copper surface atoms (e.g., steps), leaving most terraces open after annealing.

The interaction between the alumina overcoat and the copper nanoparticles was also examined with X-ray adsorption fine structure spectroscopy (EXAFS) and X-ray adsorption near edge spectroscopy (XANES). According to the XANES and EXAFS curve fits (Table S3), Cu/γ-Al_2O_3 is reduced (within accuracy of the techniques), whereas 45ALD/Cu/γ-Al_2O_3-973 is partially oxidized because of the presence of the overcoat. Furthermore, examination of used samples demonstrated that Cu/γ-Al_2O_3 sintered (i.e., copper–copper coordination increased), whereas the copper–copper coordination did not change in 45ALD/Cu/γ-Al_2O_3-973.

The surface of the copper nanoparticles was probed further using Fourier transform infrared (FTIR) spectroscopy of adsorbed CO. The main features of the IR spectra of CO adsorbed on Cu/γ-Al_2O_3 at 123 K were a band at 2099 cm^{-1}

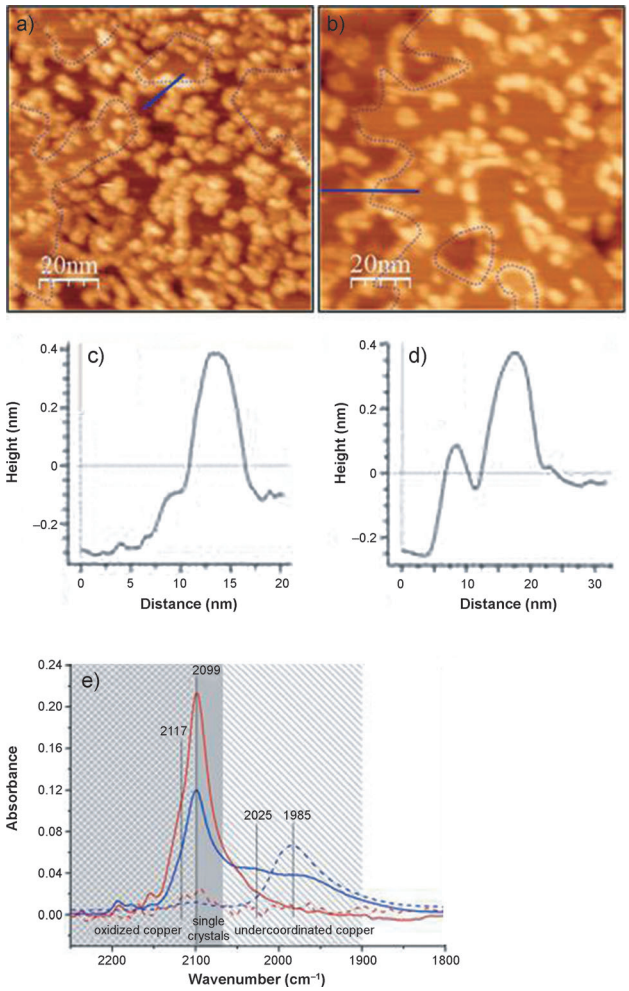

Figure 4. a) STM image of an oxidized and hydrated Cu(111) surface after four cycles of exposure to TMA and water. b) STM image after annealing at 773 K in vacuum. The dashed lines highlight the step edges. c, d) Height profiles along the solid blue lines (for a and b, respectively) indicate the position of a step edge. e) IR bands for CO adsorbed on Cu/γ-Al_2O_3 (——) and 45ALD/Cu/γ-Al_2O_3-973 (——) at 123 K (solid lines) and 283 K (dashed lines). The intensities are normalized by the pellet density and copper loading. Shaded regions indicate typical wavenumbers for CO adsorbed at different types of copper surface sites.

with a shoulder at 2117 cm^{-1} and a broad absorption at lower wavenumber (Figure 4e). The band at 2099 cm^{-1} is typical of CO adsorbed on oxide-supported copper particles. In single-crystal studies, Hollins et al. demonstrated that these bands arise from a high coverage of adsorbed CO on sites of a Cu(111) surface near (2117 cm^{-1}) and far from oxygen atoms (2099 cm^{-1}).[13] In agreement with these assignments, Kim et al. assigned bands at 2091 and 2116 cm^{-1} to CO adsorbed on a Cu(100) surface decorated with oxygen.[14] Density functional theory calculations for the stretching frequencies of CO adsorbed on various copper sites near AlO_x moieties confirmed that the CO band shifts to higher wavenumbers when the CO is located more closely to AlO_x on the surface (Figure S4). Consequently, the shoulder at 2117 cm^{-1} for Cu/γ-Al_2O_3 is assigned to adsorption of CO on copper terrace sites near the support, and the band at 2099 cm^{-1} is attributed to copper terrace sites further away from oxygen atoms. The broad absorption at lower wavenumbers is assigned to CO adsorbed to highly under-coordinated copper sites on the catalyst surface.[15] The band at 2099 cm^{-1} disappeared as the sample was warmed to 283 K, which confirms its assignment as Cu^0 and not Cu^{1+}. The broad band at lower wavenumber remained upon warming, owing to the strong binding of CO to highly under-coordinated copper sites.

The FTIR spectrum for CO adsorbed on 45ALD/Cu/γ-Al_2O_3-973 at 123 K is dominated by the band at 2099 cm^{-1}. Importantly, the relative intensity of the band at 2099 cm^{-1} compared to that of the broad absorption at lower wavenumber indicates that the highly under-coordinated copper sites that are responsible for sintering and leaching were selectively covered by the ALD overcoating procedure.

We have shown that an ALD overcoat acts to stabilize base metal nanoparticles against sintering and leaching. Calcination at high temperature opens the overcoating, exposing the copper underneath, while maintaining a stabilizing interaction with low-coordination copper sites on the surface that are prone to sintering and leaching. This strategy for stabilization should be useful in supplementing precious metal catalysts with abundant base metals for a range of traditional and bio-renewable applications where catalyst stability is a challenge, which in turn could lead to more sustainable processes. Moreover, the ability to stabilize base metals should be relevant in other precious metal applications, such as electronics and batteries.

Received: September 19, 2013
Published online: November 26, 2013

Keywords: atomic layer deposition · biomass · catalyst stability · copper · hydrogenation

[1] a) *Catalysis without Precious Metals*, Wiley-VCH, Weinheim, **2010**; b) M. V. Twigg, M. S. Spencer, *Appl. Catal. A* **2001**, *212*, 161–174; M. Twigg, M. Spencer, *Top. Catal.* **2003**, *22*, 191–203; c) M. Besson, P. Gallezot, *Catal. Today* **2003**, *81*, 547–559; d) A. I. Abdulagatov, Y. Yan, J. R. Cooper, Y. Zhang, Z. M. Gibbs, A. S. Cavanagh, R. G. Yang, Y. C. Lee, S. M. George, *ACS Appl. Mater. Interfaces* **2011**, *3*, 4593–4601.
[2] a) X. Liang, J. Li, M. Yu, C. N. McMurray, J. L. Falconer, A. W. Weimer, *ACS Catal.* **2011**, *1*, 1162–1165; b) H. Feng, J. L. Lu, P. C. Stair, J. W. Elam, *Catal. Lett.* **2011**, *141*, 512–517.
[3] J. Lu, B. Fu, M. C. Kung, G. Xiao, J. W. Elam, H. H. Kung, P. C. Stair, *Science* **2012**, *335*, 1205–1208.
[4] R. L. Puurunen, *J. Appl. Phys.* **2005**, *97*, 121301–121352.
[5] G. C. Chinchen, C. M. Hay, H. D. Vandervell, K. C. Waugh, *J. Catal.* **1987**, *103*, 79–86.
[6] K. J. Zeitsch, *The chemistry and technology of furfural and its many by-products*, *Vol. 13*, Elsevier, Amsterdam, **2000**.
[7] E. W. Hagaman, J. Jiao, B. Chen, Z. Ma, H. Yin, S. Dai, *Solid State Nucl. Magn. Reson.* **2010**, *37*, 82–90.
[8] C. Pecharromán, I. Sobrados, J. E. Iglesias, T. González-Carreño, J. Sanz, *J. Phys. Chem. B* **1999**, *103*, 6160–6170.
[9] L. B. Skinner, A. C. Barnes, P. S. Salmon, L. Hennet, H. E. Fischer, C. J. Benmore, S. Kohara, J. K. R. Weber, A. Bytchkov, M. C. Wilding, J. B. Parise, T. O. Farmer, I. Pozdnyakova, S. K. Tumber, K. Ohara, *Phys. Rev. B* **2013**, *87*, 024201.

[10] Y. J. Pagán-Torres, J. M. R. Gallo, D. Wang, H. N. Pham, J. A. Libera, C. L. Marshall, J. W. Elam, A. K. Datye, J. A. Dumesic, *ACS Catal.* **2011**, *1*, 1234 – 1245.
[11] J. Greeley, *Electrochim. Acta* **2010**, *55*, 5545 – 5550.
[12] J. Lu, B. Liu, J. P. Greeley, Z. Feng, J. A. Libera, Y. Lei, M. J. Bedzyk, P. C. Stair, J. W. Elam, *Chem. Mater.* **2012**, *24*, 2047 – 2055.
[13] P. Hollins, J. Pritchard, *Surf. Sci.* **1983**, *134*, 91 – 108.
[14] C. M. Kim, C. W. Yi, D. W. Goodman, *J. Phys. Chem. B* **2005**, *109*, 1891 – 1895.
[15] a) F. Boccuzzi, G. Ghiotti, A. Chiorino, *Surf. Sci.* **1985**, *156* (Part 2), 933 – 942; b) G. Ghiotti, F. Boccuzzi, A. Chiorino, *Stud. Surf. Sci. Catal.* **1985**, *21*, 235 – 246; c) K. Hadjiivanov, T. Venkov, H. Knözinger, *Catal. Lett.* **2001**, *75*, 55 – 59.

